Solvatochromism in Perylene Diimides; Experiment and Theory

Fuller, C. A.; Finlayson, Christopher

Published in:
Physical Chemistry Chemical Physics

DOI:
10.1039/C7CP05039A

Publication date:
2017

Citation for published version (APA):
Fuller, C. A., & Finlayson, C. (2017). Solvatochromism in Perylene Diimides; Experiment and Theory. *Physical Chemistry Chemical Physics*, *19*(47), 31781-31787. [31781]. https://doi.org/10.1039/C7CP05039A

PCCP

Accepted Manuscript

This article can be cited before page numbers have been issued, to do this please use: C. A. Fuller and C. E. Finlayson, *Phys. Chem. Chem. Phys.*, 2017, DOI: 10.1039/C7CP05039A.

ROYAL SOCIETY OF CHEMISTRY

rsc.li/pccp

View Article Online
DOI: 10.1039/C7CP05039A

PCCP

ARTICLE

Solvatochromism in Perylene Diimides; Experiment and Theory

C. A. Fuller,[a,†] and C. E. Finlayson[a,*]

Received 00th January 20xx,
Accepted 00th January 20xx

DOI: 10.1039/x0xx00000x

www.rsc.org/

We report an experimental and computational investigation into the solvatochromism of a perylene diimide derivative. The alkyl swallowtail substituents allowed solubility in many solvents of widely differing polarity, with a complicated resultant behaviour, illustrating both negative and positive solvatochromism as a function of dielectric constant. Luminescence quantum yield and optical absorption linewidth displayed an inverse correlation, indicating varying degrees of intermolecular aggregation, and a remarkably similar trend was found between the peak absorption wavelength and the solvent boiling point, illustrating the dependency of aggregation on the solvent interactions. These outline trends may be parameterised by an empirically derived dimensionless quantity, as a tool to be used in more sophisticated future models of solvatochromism in small molecule chromophores.

Introduction

Perylene molecules are a class of semiconducting polycyclic aromatic hydrocarbons with the empirical formula $C_{20}H_{12}$.[1] Due to their favourable photophysical properties, stable n-type semiconducting properties, and chemical versatility, perylene diimides (PDI) in particular have gathered interest in recent years. It is possible to chemically modify the PDI structure by introducing peripheral substituents, allowing modulation of inter- and intramolecular forces, thus molecules of significantly different optical, electronic and conformal properties may be tailored.[2, 3] Furthermore, PDIs and their derivatives have become increasingly well-recognised materials for use in photovoltaics, organic light emitting diodes and organic thin-film transistors.[4-8] Further optmisation of the electronic and optical properties of PDIs holds potential for improved device performance. Developments in supramolecular chemistry have also yielded numerous examples of the use of PDIs as moities and modular components in engineered arrays, with advanced photophysical, optical and electronic functionality.[9-13]

The rigid aromatic core of many perylene derivatives favour π-π intermolecular interactions. The planar π-conjugated core of PDI molecules are typically characterised by strong π-π stacking, which can play a key role in J- and H-aggregation and self assembly.[6, 14] The complex nature of these processes involves different types of intermolecular forces, including hydrogen bonding, van der waals, and ligand interactions, depending on the system of molecules.[13, 14] The ability to modify the PDI cores by adding substituents can induce various effects on the packing structures;[15, 16] molecular groups may be bonded to each of the outlying carbon atoms, where sections of the core are aptly named the peri, bay and ortho-positions, and a detailed study of this was reported by Li *et al.*[2] Alterations to the peri-positions tend to exclusively affect solubility and aggregation of PDIs, thus the focus of this investigation was therefore towards solvation behaviour and associated photophysical trends. The PDI molecules studied here are shown in Figure 1; material X, where C_6 alkyl swallowtail substituents are located on the N-terminal of the imide group at the peri-position of the perylene core, and material Y, where bulkier cargoes featuring three C_{12} alkoxy side chains are positioned on the N-terminals.

Kasha and others have developed a classification of H- and J-type aggregation, relating photophysical roles and morphology in molecular assemblies.[17-19] Compared to the monomer emission, the head-to-tail structure of J-aggregates often exhibit high luminescence quantum yields. By contrast, the face-to-face stacked structures of H-aggregates are commonly associated with strong quenching.

Figure 1; schematics of the chemical structures of the perylene-diimides (PDIs) being studied, denoted as materials X and Y as indicated. The clear solvatochromism of PDIs is shown (top inset), as material X is dissolved in a range of differing solvents.

[a] *Dept of Physics, Prifysgol Aberystwyth University, Wales SY23 3BZ, U.K. E-mail; cef2@aber.ac.uk*
† Presently at; Centre for Doctoral Training in Plastic Electronics, Imperial College, London SW7 2BZ, U.K.

View Article Online
DOI: 10.1039/C7CP05039A

Generally, a bathochromic absorption band shift signals the presence of J-type aggregation, due to the formation of low energy absorption bands (conversely, higher-energy, hypsochromic bands result from H-type). J-aggregates are also associated with a narrow absorption band and a small Stokes shift, whereas the line-shapes of H-aggregates are more complicated due to the complex vibronic structure of organic dyes. Whilst the trends of H- and J-bands contrast, molecules have displayed both qualities simultaneously,[20] and the versatility of PDI derivatives means that H- or J- aggregates may be formed for a given molecule depending on the added substituents and, critically, the nature of the solvent.[18, 21] Whilst these studies have focused on the influence of aggregation, other models have proposed other mechanisms, such as competition between structural change and intramolecular charge transfer,[22] particularly in molecules liable to exhibit a zwitterionic character.[23]

This study characterises, compares, and models the optical properties of a particular PDI derivatives (as described) with an emphasis on solvatochromic behaviour and trends in a range of solvent media Measurements show an unusual overall behaviour as a function of dielectric constant, with regimes of both negative and positive solvatochromism, for which we develop an intuitive empirical model based on how the physical properties of solvents may influence the nature of aggregation. A detailed quantum computational study of the electronic states of the molecule was also conducted, using suitable molecule-solvent interaction models, offering a qualitative insight into the significance of molecule-molecule interactions beyond these simulations.

Methodology

The wide-ranging solubility of the PDI derivative X allowed for a deeper analysis of the trends associated with aggregation and solvatochromism, whereby the molecule was dissolved into six solvents of varying dielectric constant ε (toluene ε = 2.38, chloroform 4.81, ortho-dichlorobenzene/o-DCB 9.93, acetone 20.7, acetonitrile 37.5, dimethylsulphoxide/DMSO 46.7); all solvents used were purchased from Sigma-Aldrich (UK). As shown is the image in Figure 1 (inset) the solvatochromic effect is readily observable to the naked eye. Comparable measurements were also made with PDI derivative Y, albeit within its narrower range of solubility (ε = 2.38 to 9.93).

Optical absorption spectra were measured under ambient conditions using a Red Tide UV-VIS Spectrometer (Ocean Optics) with deuterium (UV) and tungsten (visible) light sources, which produced a broadband white-light spectrum from λ = 220 to
850 nm. Spectra were fully corrected for both dark noise and reference baseline for each solvent medium used. Sample solutions were prepared in 3.5mL cuvettes, path length 1 cm with relatively low concentrations (range of $<10^{-6}$ M) used to avoid any saturation and re-absorption effects in the measured optical spectra. Critically for the present study of solvatochromism, this regime of concentration was such that

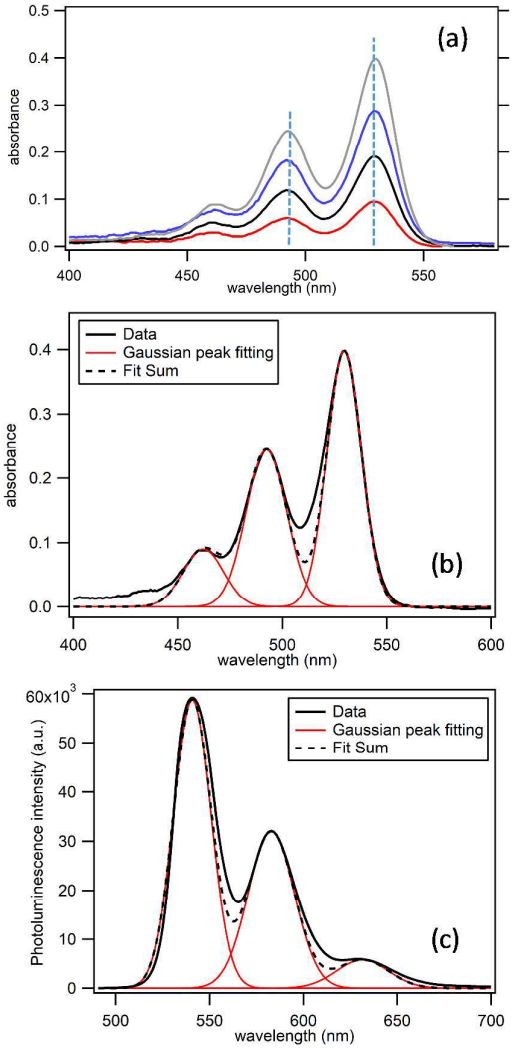

the principle absorption spectral features were not observed to vary as a function of dilution (see Figure 2a).

Figure 2; (a) Invariance of the absorption spectra of PDI material X as a function of increasing concentration in the $<10^{-6}$ M regime in ortho-dichlorobenzene (o-DCB). Fitting of experimental data; (b) optical absorbance and (c) photoluminescence of X in o-DCB, with the sum of the three fitted Gaussian peaks is shown in each case as indicated.

The sample fluorescence (photoluminescence, PL) in various solvents was measured using a diode-pumped solid-state (DPSS) laser photo-excitation source (λ = 473 nm, power ≈ 2 mW) with solutions and cuvettes in a fixed geometry, and at a fixed distance from the source. The emitted PL was collected at 90° to the incident light, using a fibre-coupled USB2000+ CCD Spectrometer (Ocean Optics). A direct method of measuring photoluminescence quantum yield (PL-QY) was employed, whereby a reference sample of known quantum efficiency was used as a comparison;[24, 25] the dye Rhodamine 6G was chosen as the reference as it absorbs in a similar region of the spectrum to the PDI molecule, as is well characterised. With the optical spectra of both the reference and PDI solution in a given solvent, the following equation was applied:

View Article Online
DOI: 10.1039/C7CP05039A
PCCP Paper

$$\Phi = \Phi_R \frac{X}{X_R} \frac{1-10^{-A_R}}{1-10^{-A}} \frac{n^2}{{n_R}^2} \quad (1)$$

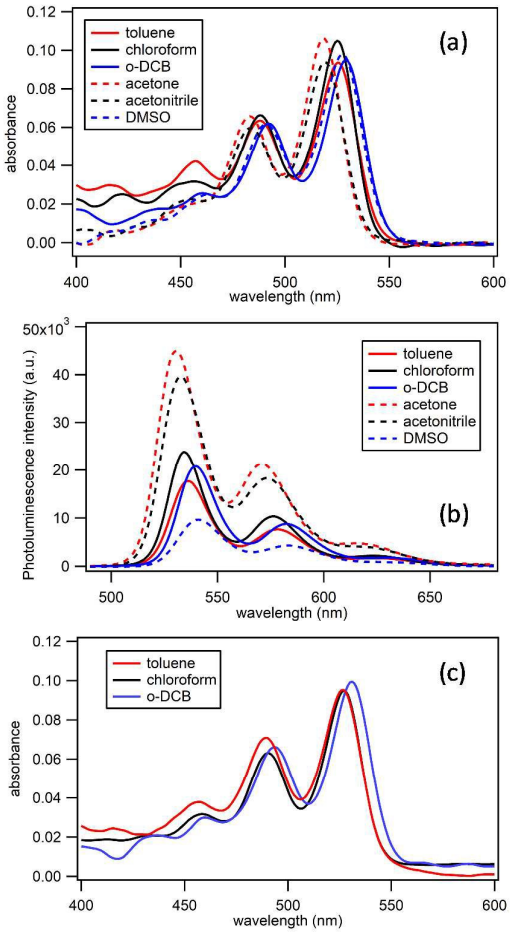

Figure 3; (a) absorption and (b) photoluminescence spectra of the PDI material X in each of the solvents studied, as indicated. All solutions were prepared in the concentration range of $<10^{-6}$ M. (c) shows corresponding absorption spectra for material Y in the 3 tractable solvents used.

where 'Φ' is the quantum yield, 'X' is the integrated area under the emission peak; 'A' is the absorbance at the excitation wavelength, and 'n' is the refractive index of the solvent. Each subscript 'R' refers to the respective values of the reference standard.[26] The determined statistical error from multiple propagations for each quantum yield calculation was approximated to be ±5%.

Quantum chemical simulations were performed using the Gaussian 09[‡] software, with the GaussView[§] graphical user interface. A relatively demanding basis set 6-31+G with the B3LYP functional was chosen for simulations, as it have shown to yield computationally tractable yet accurate results.[27] The ground-state/excited-state geometries of the molecule were optimised using the DFT/TD-DFT methods. All alkyl side-groups were removed prior to simulations as a computational necessity; such groups have a negligible influence on the core orbitals, whilst significantly extending the time taken for a convergent simulation output.[28] Frequency simulations were

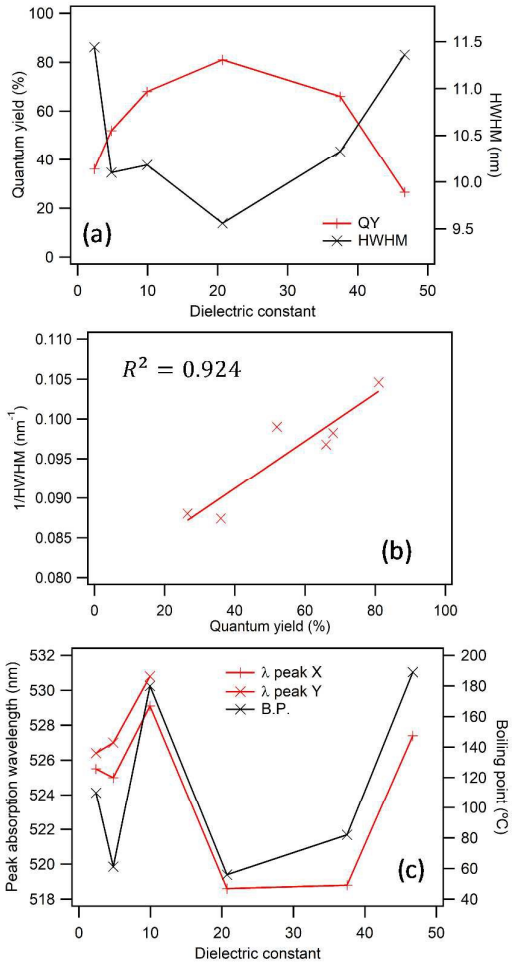

Figure 4; (a) Quantum yield and HWHM of the optical absorption spectra for PDI material X in various solutions. (b) The inverse correlation of Quantum yield and HWHM is illustrated, together with a regression analysis. (c) The absorption wavelength maxima in various solutions and the boiling point of the respective solvent; comparative data for material Y is shown as indicated.

calculated for the ground and excited-states to enable further detailed simulation of the vibrationally resolved absorption spectrum, providing an additional gauge of the efficacy level of the simulation methods employed.[29] The methodologies followed those in the software technical report in GAUSSIAN 09, Revision A.02; namely, "Vibrationally-resolved electronic spectra in GAUSSIAN 09", by V. Barone, J. Bloino, M. Biczysko.[#]

Results and discussion

Experimental results

As shown in Figure 2b, the characteristic absorption spectrum of material X exhibits the 0-0, 0-1 and 0-2 vibrational mode

View Article Online
DOI: 10.1039/C7CP05039A

transitions of the S_0-S_1 electronic transition, in common with such planar π-conjugated organic molecules.[10, 30] A relatively small Stokes shift was measured in the range of 10 nm, as is a common trait of spectra with the most intense peak corresponding to the 0-0 transition. In Figure 2c, the PL and absorption spectra are mirrored with three peaks being resolvable, as per the Franck-Condon principle.[30]

In Figure 3, the solvatochromism of the PDI material X is shown spectroscopically, with both the absorption and PL showing significant variation in the solvents studied, as collated in Table 1. Extracting the trend of the 0-0 transition peak wavelength against solvent dielectric constant shows a general
trend of hypsochromism in the low to mid ε range, and a reversed trend of bathochromism in the mid to high ε range (see Figure 4c). We note the broad similarity of these behaviours to those reported earlier by Zoon and Brouwer.[31] A similarly interesting correlation was found between the quantum yield and half-width half maximum (HWHM) of absorption maxima bands as a function of the dielectric constant of the solvent medium (see Figure 4a).

As the trends of solvatochromism do not follow the simple bathochromic relationship expected from solvent-molecule interactions,[32] these results suggest a varying degree of aggregation, and aggregation mechanisms, driven by changes in solvent polarity. Further analysis of this will be described in the simulations below. J-aggregates, in particular, are characterised by narrow absorption bands and high quantum yields, which correlates well with J-aggregation effects being most evident in Acetone (ε = 20.7). In addition to this, the higher degree of quenching in most solutions may indicate the presence of some H-type aggregation. Thus a more complex system of supramolecular structures is considered, whereby both species-type may be co-existent.

Furthermore, it is clear that the π–π stacking of these aromatic molecules is strongly influenced by the solvent, a result consistent with previous studies.[16, 33] We might consider such molecule-molecule interactions may be influenced by the intermolecular forces (e.g. Van der Waals) in the solution media. A marked correlation was found empirically between the absorption wavelength maxima and the boiling point of its respective solvent; this is highlighted in Figure 4c, showing evidence of the significant influence solvent polarity has on the behaviour of aggregated PDI molecules in solution. It is hypothesised that the complex group of intermolecular forces which are responsible for the solvent boiling point also influence these aggregated PDI molecules in solution, resulting in the similarities between the two. The wavelength shifts are thought to correspond to aggregation fluctuations, whereby different solvents will cause the PDI molecules to form different aggregated structures.

Modelling and Simulations results

A universal model predicting solvatochromic shifts may prove useful in this field and perhaps could be implemented in computational simulation methods. Thus an elementary model, both intuitive and semi-empirical, is devised here to describe the solvatochromic variations, using parameters commonly associated with solubility and boiling point values. A degree of correlation between solvatochromism and molecular dipole moment has been observed in previous articles, and further study found that various other solvent parameters broadly matched this unique trend, such as the density and molecular weight.[3] As a result, an attempt to derive a simple equation-based model, which linked the boiling point and wavelength shift, via a standard dimensional analysis of these key parameters, is developed.

Table 1; key parameters from optical characterisation of PDI, in solvents of differing dielectric constant ε. These are fitted absorption peaks (λ_{abs}), photoluminescence peaks (λ_{PL}), Stokes shift and photoluminescence quantum-yield (PL-QY) for material X, with comparable absorption data also shown for material Y.

	ε	λ_{abs} (nm)	λ_{abs} (nm) material Y	λ_{PL} (nm)	Stokes (nm)	PL-QY(%)
Toluene	2.38	525.2 488.6 456.1	526.3 489.2 456.7	537.0 578.3 624.7	12.0	36
Chloroform	4.81	525.0 488.2 452.4	527.0 490.0 458.5	534.0 576.6 624.7	9.0	52
o-DCB	9.93	529.0 492.2 460.0	530.8 493.4 459.4	540.5 582.0 630.3	15.5	68
Acetone	20.7	518.6 483.0 450.8		530.8 570.7 617.2	12.2	81
Acetonitrile	37.5	518.8 483.6 451.9		533.1 573.0 618.2	14.3	66
DMSO	46.7	524.7 490.9 461.5		541.2 583.1 634.2	16.5	27

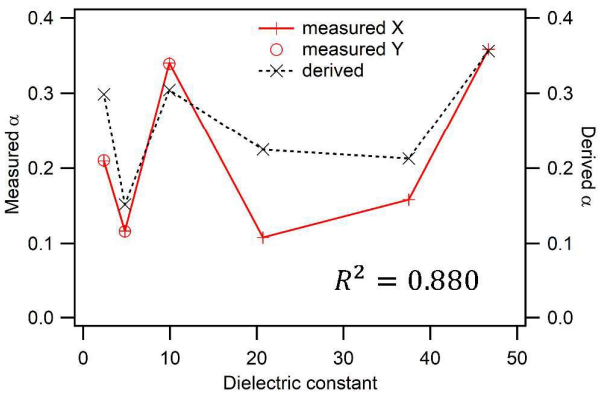

Figure 5; The measured values for the ratio between the absorption wavelength maxima and solvent boiling point for both PDI materials X and Y, as compared to the derived parameter α.

The mathematical expression is based on the dielectric constant (ε), density (ρ), molar mass (M_m), molar concentration (c_m) and dipole moment for the molecule (D_m)

View Article Online
DOI: 10.1039/C7CP05039A
PCCP Paper

and each solvent (D_{ms}).[§§] These terms were chosen by dimensional analysis to give a derived dimensionless parameter (α_d), i.e.

$$\alpha_d = \frac{M_m \times \varepsilon \times c_m \times D_m}{D_{ms} \times \rho} \qquad (2)$$

Comparing this expression to the experimental results, where alpha (α) represents the boiling point divided by absorption maxima wavelength, yields a similar trend as shown in Figure 5. The results obtained for material Y also shown an excellent quantitative agreement, over the limited range over which data is collected, giving some initial indications of the potential applicability of our model and approach. Whilst this model still lacks some intuitive components, such as explicit parameters relating to the solute and the temperature dependence of the dielectric constant, it demonstrably offers a good starting point as a predictive tool, for development into more sophisticated models of solvatochromism in small molecule semiconductors, such as the PDIs. We note that a closer study of temperature dependence might enable a convergence with other physical models of intermolecular interactions, such as the Hildebrand solubility parameter (δ),[34] which is related to the square root of the cohesive energy density (heat of vaporisation per molar volume) of solution.

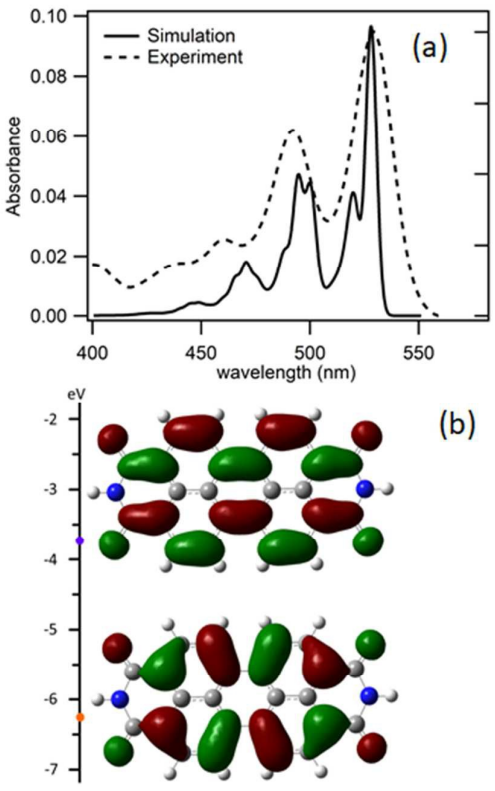

Figure 6; (a) Experimental absorption spectra for PDI material X in toluene, in comparison to the quantum chemical simulation. (b) LUMO (top, purple) and HOMO (bottom, orange); calculated energies and orbitals for the optimised simulation.

The PDI material X was found to be simulation-friendly, allowing the vibronically resolved spectra to be accurately simulated in Gaussian (Figure 6a). The resulting absorption spectrum shows features very similar to the experimentally collected data for the PDI in toluene; the line-shape is broadly accurate and shows additional fine structure which is broadened out experimentally. The simulated HOMO and LUMO electronic wavefunctions are also representative of PDI molecules, with these orbitals being focused on the perylene inner core (Figure 6b). The corresponding calculated energy gap (≈ 2.4 eV) calculated indicated that the spectral features observed both experimentally and computationally exclusively originate from the HOMO-LUMO transition, as expected.

Finally, the effects of medium dielectric constant on the electronic and optical molecule were simulated with Gaussian, using the methods described above in the *Methodology* section, and a Polarizable Continuum Model (PCM) from Self-Consistent Reaction Field (SCRF) solvation theory;[35] the results of this are summarised in Table 2. For the simulation in "free-space" gas-phase, it is implicit that ε = 1. We observe the calculated values of HOMO and LUMO both increase monotonically in magnitude (becoming more negative) with increasing ε. Likewise, the inferred 0-0 transition wavelength also increases monotonically (spanning an expected range of λ = 565 to 579 nm) with increasing ε. Hence, there is a very clear contrast with the theoretically predicted behaviour, when primarily considering the solvent-molecule interactions, and experimentally where the additional effects of intermolecular (π-π orbital) interactions must also be considered.

Table 2; quantum chemical modelling outputs, giving calculated solvation energies (E_{solv}), HOMO/LUMO energies, predicted absorption wavelength (λ_{peak}), and dimensionless 0-0 oscillator strength (f_i), in each of the solvent media studied.

	E_{solv} (KJ/mol)	HOMO (eV)	LUMO (eV)	λ_{peak} (nm)	f_i
Free space	-	-6.37	-4.18	565.4	0.659
Toluene	44.6	-6.25	-4.08	571.3	0.866
Chloroform	68.1	-6.19	-4.04	574.9	0.976
o-DCB	83.9	-6.15	-4.00	577.7	1.048
Acetone	91.7	-6.13	-3.99	579.0	1.084
Acetonitrile	96.9	-6.12	-3.98	579.6	1.100
DMSO	96.9	-6.12	-3.98	579.7	1.105

Conclusions

In this experimental and computational investigation into the solvatochromism of a perylene diimide derivative, a complicated general trend of hypsochromism in the low to mid ε range, and a reversed trend of bathochromism in the mid to high ε range, was observed. The dependency of aggregation on the solvent interactions and polarities was illustrated by the inverse correlations between luminescence quantum yield and absorption linewidth, and also the peak absorption wavelength and the solvent boiling point.

View Article Online
DOI: 10.1039/C7CP05039A

A detailed quantum computational study of the electronic states of the molecule was also conducted, including suitable solvation models, offering a qualitative insight into the significance of intermolecular π–π interactions beyond the solvent interactions in these simulations. In contrast to experimental observation, the calculated values of HOMO, LUMO, and the inferred peak absorption wavelength all vary monotonically with increasing ε. An elementary intuitive model was thus developed, which successfully links the solvatochromic variations with physical parameters associated with intermolecular forces within the solvent media, such as solubility and boiling point.

With perylene chromophores and derivatives currently such an important class of functional materials in soft- and solution-state media, covering the diverse fields of biomedicinal photosensitizers,[36, 37] fluorescent labelling/imaging agents,[38, 39] drug carrying nanomaterials,[40] diagnostic agents and molecular probes[41] (in addition to their putative uses in organic optoelectronics as described previously), this work points towards improved empirical models of solvatochromism effects in small molecule chromophores.

Acknowledgements

The PDI materials studied in this paper originated from the group of Prof. Paul Kouwer, Radboud University Nijmegen. The authors thank Dr Edwin Flikkema (Aberystwyth University) and Dr Sebastian Albert-Seifried for helpful discussions. CEF acknowledges the support of a *University Research Fund* (URF) grant from Aberystwyth University.

Notes and references

‡ Gaussian 09, Revision E.01; M. J. Frisch, G. W. Trucks, H. B. Schlegel, G. E. Scuseria, M. A. Robb, J. R. Cheeseman, G. Scalmani, V. Barone, G. A. Petersson, H. Nakatsuji, X. Li, M. Caricato, A. Marenich, J. Bloino, B. G. Janesko, R. Gomperts, B. Mennucci, H. P. Hratchian, J. V. Ortiz, A. F. Izmaylov, J. L. Sonnenberg, D. Williams-Young, F. Ding, F. Lipparini, F. Egidi, J. Goings, B. Peng, A. Petrone, T. Henderson, D. Ranasinghe, V. G. Zakrzewski, J. Gao, N. Rega, G. Zheng, W. Liang, M. Hada, M. Ehara, K. Toyota, R. Fukuda, J. Hasegawa, M. Ishida, T. Nakajima, Y. Honda, O. Kitao, H. Nakai, T. Vreven, K. Throssell, J. A. Montgomery, Jr., J. E. Peralta, F. Ogliaro, M. Bearpark, J. J. Heyd, E. Brothers, K. N. Kudin, V. N. Staroverov, T. Keith, R. Kobayashi, J. Normand, K. Raghavachari, A. Rendell, J. C. Burant, S. S. Iyengar, J. Tomasi, M. Cossi, J. M. Millam, M. Klene, C. Adamo, R. Cammi, J. W. Ochterski, R. L. Martin, K. Morokuma, O. Farkas, J. B. Foresman, and D. J. Fox, Gaussian, Inc., Wallingford CT, 2016.

§ GaussView, Version 5; R. Dennington, T. A. Keith, and J. M. Millam, Semichem Inc., Shawnee Mission, KS, 2016.

The Gaussian input file used for the generated vibrational spectrum (space sensitive):

Link 0 Commands
- %Chk=Perylene_GS
- #P Geometry=AllCheck Frequency=(ReadFC,FC,SaveNM) NoSymm
- %Chk=Perylene_EES

The GaussView level of theory used for each ground state and excited state calculation:
- GS: #p opt freq=savenormalmodes b3lyp/6-31(d) geom=connectivity
- EES: #p opt freq=savenormalmodes td=(nstates=10) b3lyp/6-31(d) geom=connectivity

§§ The values used for these terms may be obtained from *CRC Handbook of Chemistry and Physics* (97th edition, 2016), W.M. Haynes (Editor), CRC Press, UK

1. D. DONALDSON, J. ROBERTSON and J. WHITE, *Proceedings of the Royal Society of London Series a-Mathematical and Physical Sciences*, 1953, **220**, 311-321.
2. C. Li and H. Wonneberger, *Advanced Materials*, 2012, **24**, 613-636.
3. M. Farooqi, M. Penick, J. Burch, G. Negrete and L. Brancaleon, *Spectrochimica Acta Part a-Molecular and Biomolecular Spectroscopy*, 2016, **153**, 124-131.
4. C. Struijk, A. Sieval, J. Dakhorst, M. van Dijk, P. Kimkes, R. Koehorst, H. Donker, T. Schaafsma, S. Picken, A. van de Craats, J. Warman, H. Zuilhof and E. Sudholter, *Journal of the American Chemical Society*, 2000, **122**, 11057-11066.
5. E. Kozma and M. Catellani, *Dyes and Pigments*, 2013, **98**, 160-179.
6. E. Kozma, W. Mroz, F. Villafiorita-Monteleone, F. Galeotti, A. Andicsova-Eckstein, M. Catellani and C. Botta, *Rsc Advances*, 2016, **6**, 61175-61179.
7. D. Sun, D. Meng, Y. Cai, B. Fan, Y. Li, W. Jiang, L. Huo, Y. Sun and Z. Wang, *Journal of the American Chemical Society*, 2015, **137**, 11156-11162.
8. D. Meng, D. Sun, C. Zhong, T. Liu, B. Fan, L. Huo, Y. Li, W. Jiang, H. Choi, T. Kim, J. Kim, Y. Sun, Z. Wang and A. Heeger, *Journal of the American Chemical Society*, 2016, **138**, 375-380.
9. C. Finlayson, R. Friend, M. Otten, E. Schwartz, J. Cornelissen, R. Nolte, A. Rowan, P. Samori, V. Palermo, A. Liscio, K. Peneva, K. Mullen, S. Trapani and D. Beljonne, *Advanced Functional Materials*, 2008, **18**, 3947-3955.
10. E. Schwartz, V. Palermo, C. Finlayson, Y. Huang, M. Otten, A. Liscio, S. Trapani, I. Gonzalez-Valls, P. Brocorens, J. Cornelissen, K. Peneva, K. Mullen, F. Spano, A. Yartsev, S. Westenhoff, R. Friend, D. Beljonne, R. Nolte, P. Samori and A. Rowan, *Chemistry-a European Journal*, 2009, **15**, 2536-2547.
11. S. Albert-Seifried, C. Finlayson, F. Laquai, R. Friend, T. Swager, P. Kouwer, M. Juricek, H. Kitto, S. Valster, R. Nolte and A. Rowan, *Chemistry-a European Journal*, 2010, **16**, 10021-10029.
12. Y. Huang, X. Yang, E. Schwartz, L. Lu, S. Albert-Seifried, C. Finlayson, M. Koepf, H. Kitto, B. Ulgut, M. Otten, J. Cornelissen, R. Nolte, A. Rowan and R. Friend, *Journal of Physical Chemistry B*, 2011, **115**, 1590-1600.
13. F. Wurthner, *Chemical Communications*, 2004, 1564-1579.
14. Z. Chen, V. Stepanenko, V. Dehm, P. Prins, L. Siebbeles, J. Seibt, P. Marquetand, V. Engel and F. Wurthner, *Chemistry-a European Journal*, 2007, **13**, 436-449.
15. A. Namepetra, E. Kitching, A. Eftaiha, I. Hill and G. Welch, *Physical Chemistry Chemical Physics*, 2016, **18**, 12476-12485.
16. Z. Chen, B. Fimmel and F. Wurthner, *Organic & Biomolecular Chemistry*, 2012, **10**, 5845-5855.

View Article Online
DOI: 10.1039/C7CP05039A
PCCP Paper

17. K. Kistler, C. Pochas, H. Yamagata, S. Matsika and F. Spano, *Journal of Physical Chemistry B*, 2012, **116**, 77-86.
18. A. Eisfeld and J. Briggs, *Chemical Physics*, 2006, **324**, 376-384.
19. N. Hestand and F. Spano, *Journal of Chemical Physics*, 2015, **143**.
20. A. Sarbu, L. Biniek, J. Guenet, P. Mesini and M. Brinkmann, *Journal of Materials Chemistry C*, 2015, **3**, 1235-1242.
21. S. Ghosh, X. Li, V. Stepanenko and F. Wurthner, *Chemistry-a European Journal*, 2008, **14**, 11343-11357.
22. V. Manzoni, K. Coutinho and S. Canuto, *Chemical Physics Letters*, 2016, **655**, 30-34.
23. C. Martins, M. Lima, E. Bastos and O. El Seoud, *European Journal of Organic Chemistry*, 2008, 1165-1180.
24. J. R. Lakowicz, in *Principles of Fluorescence Spectroscopy (3rd ed.)*, Springer, USA, 2006, pp. 55-56.
25. C. E. Finlayson, A. Amezcua, P. J. A. Sazio, P. S. Walker, M. C. Grossel, R. J. Curry, D. C. Smith and J. J. Baumberg, *Journal of Modern Optics*, 2005, **52**, 955-964.
26. A. Brouwer, *Pure and Applied Chemistry*, 2011, **83**, 2213-2228.
27. C. Adamo and D. Jacquemin, *Chemical Society Reviews*, 2013, **42**, 845-856.
28. J. High, K. Virgil and E. Jakubikova, *Journal of Physical Chemistry a*, 2015, **119**, 9879-9888.
29. V. Barone, J. Bloino, M. Biczysko and F. Santoro, *Journal of Chemical Theory and Computation*, 2009, **5**, 540-554.
30. M. Sauer, J. Hofkens and J. Enderlein, in *Handbook of Fluorescence Spectroscopy and Imaging: From Single Molecules to Ensembles.*, Wiley-VCH, Weinheim, Germany, 2011.
31. P. Zoon and A. Brouwer, *Chemphyschem*, 2005, **6**, 1574-1580.
32. C. Reichardt and T. Welton, in *Solvents and solvent effects in organic chemistry*, Wiley-VCH, Weinheim, Germany, 2010, p. 360.
33. F. Wurthner, C. Thalacker, S. Diele and C. Tschierske, *Chemistry-a European Journal*, 2001, **7**, 2245-2253.
34. A. F. M. Barton, in *CRC Handbook of Solubility Parameters and Other Cohesion Parameters*, CRC Press, Boca Raton, FL, USA, 2nd edn., 1991.
35. J. Tomasi, B. Mennucci and R. Cammi, *Chemical Reviews*, 2005, **105**, 2999-3093.
36. W. Xu, H. Chen, Y. Wang, C. Zhao, X. Li, S. Wang and Y. Weng, *Chemphyschem*, 2008, **9**, 1409-1415.
37. B. Gao, Y. Liu, H. Yin, Y. Li, Q. Bai and L. Zhang, *New Journal of Chemistry*, 2012, **36**, 28-31.
38. T. Heek, C. Fasting, C. Rest, X. Zhang, F. Wurthner and R. Haag, *Chemical Communications*, 2010, **46**, 1884-1886.
39. B. Gao, H. Li, H. Liu, L. Zhang, Q. Bai and X. Ba, *Chemical Communications*, 2011, **47**, 3894-3896.
40. A. Jana, K. Nguyen, X. Li, P. Zhu, N. Tan, H. Agren and Y. Zhao, *Acs Nano*, 2014, **8**, 5939-5952.
41. N. Sikdar, D. Dutta, R. Haldar, T. Ray, A. Hazra, A. Bhattacharyya and T. Maji, *Journal of Physical Chemistry C*, 2016, **120**, 13622-13629.